TAO, Vol. 9, No. 3, 379-393, September 1998

Crustal Velocity Variation of the Western Philippine Sea Plate From TAICRUST OBS/MCS Line 23

Yi-Shyue Yang[1] and Tan K. Wang[1]

(Manuscript received 7 January 1998, in final form 27 August 1998)

ABSTRACT

The aims of this research are to understand the deformation of the shallow structures (<6 km depth), the crustal velocity variation of the western Philippine Sea Plate (PSP) and their relation to the arc-continent collision using Ocean Bottom Seismometers (OBS) and a multi-channel seismic (MCS) survey (together known as TAICRUST) offshore southeastern Taiwan. A seismic line, Line 23 which covers the Luzon Arc, the Huatung Basin, the Taitung Canyon and the western edge of the Gagua Ridge, is investigated. Prominent reflected and refracted arrivals from the sediment, the oceanic basement and the Moho can be seen in the OBS data. By applying the travel-time inversion of the stacked MCS data and the OBS data, the velocity-depth model is built sequentially from the shallow to the deep structures. Low RMS travel-time error and numerous travel-time picks demonstrate the accuracy and the high resolution of the model, respectively.

A deep basement beneath OBS stations 30 and 31, a narrow basement trough beneath the Taitung Canyon, and the long-wavelength bending of the oceanic crust near the western edge of the Gagua Ridge are found in the velocity model. Anomalously low velocity in the upper crust is also identified beneath the Taitung Canyon and near the Gagua Ridge. The former may result from the strike-slip fault while the latter may be generated from the uplift of the Gagua Ridge. According to the variation of the crustal thickness, the velocity model is divided into three portions with the distance larger than 74 km, between 23 and 74 km, and less than 23 km from its northwest end. The crustal thickness in the southeast portion (>74 km) is almost uniform at about 12 km. Similarly, the thickness of the upper crust in the central model (23~74 km) and the thickness of the lower crust in the northwest portion (<23 km) remain uniform at about 4 km and 8 km, respectively. However, the lower crust in the central portion and the upper crust in the northwest portion gradually thicken northwestward. The maximum crustal thickness is about 24 km at the northwest end of the velocity model. The variations of the crustal thickness and the lateral velocity at a

[1] Institute of Applied Geophysics, National Taiwan Ocean University, Keelung, Taiwan, 20224, ROC

distance of 23 km from the northwest end of the model imply the eastern edge of the Luzon Arc. Furthermore, northwestward dipping of the Moho in the velocity model is consistent with other studies. The mechanism of crustal thickening in the western PSP is probably related to intra-plate deformation, thrust faulting and/or future subduction of the western PSP beneath the Luzon Arc.

(Key words: Crustal variation, OBS, Travel-time inversion, Philippine Sea Plate, Luzon Arc, Moho, Depression)

1. INTRODUCTION

Taiwan is located in a complex and tectonically active region where the western Philippine Sea Plate (PSP) is subducting northwestward below the western Ryukyu Arc while the Eurasian Plate (EP) is subducting eastward along the Manila Trench as illustrated in the upper right corner of Figure 1. At present, offshore southeastern Taiwan, the western PSP converges with the EP at a rate of 7.1 cm/yr. and along an azimuth of 310° (Seno *et al.*, 1993). Collision of the western PSP and the margin of the EP has resulted in both the northward extension of the Luzon volcanic arc and the emergence of the Coastal Range (Ho, 1988). Deformation may have accumulated within the Luzon Arc owing to arc-continent collision, but how has it further affected the basement of the western PSP and where is the eastern edge of the Luzon Arc? More geophysical data are required to determine the crustal structure beneath the western PSP and for a better understanding of the collision of the Luzon Arc and the EP.

Numerous geophysical surveys have been carried out offshore southeastern Taiwan. Earthquake tomography (Rau and Wu, 1995) provided a general trend of the tectonic structures without good constraints of the marine structures. By considering the high-resolution bathymetric data within the Huatung Basin, both the depth of the Taitung Canyon (extending from Lanyu and Lutao islands to the Ryukyu Trench for a distance of 170 km) and the elevation of the Gagua Ridge (along the 123°E meridian) were identified (Schnürle *et al.*, 1998). According to the gravity signature, the Gagua Ridge appears to be an uplifted block of the oceanic crust formed under highly oblique convergence (Karp *et al.*, 1997; Deschamps *et al.*, 1997; Hsu *et al.*, 1998) that may explain the bending of the oceanic crust near the Gagua Ridge. However, bathymetry and gravity modeling are generally insufficient to interpret the deep structures of the western PSP. Two fracture zones trending NS along 122.5°E and beneath the Taitung Canyon (as an active right-lateral strike-slip fault) have been inferred, respectively, from magnetic lineations (Hsu *et al.*, 1998) and from focal mechanisms (Sibuet and Hsu, 1997). However, more evidence is required to better define these fracture zones in crustal structures.

Previous geophysical surveys offshore southeastern Taiwan have generally provided the tectonic structures with either low resolution or high non-uniqueness. Therefore, deep seismic surveys, using large sources and seismic lines with a long offset, are required to explore deep structures in this area. A comprehensive seismic survey (known as TAICRUST) was carried

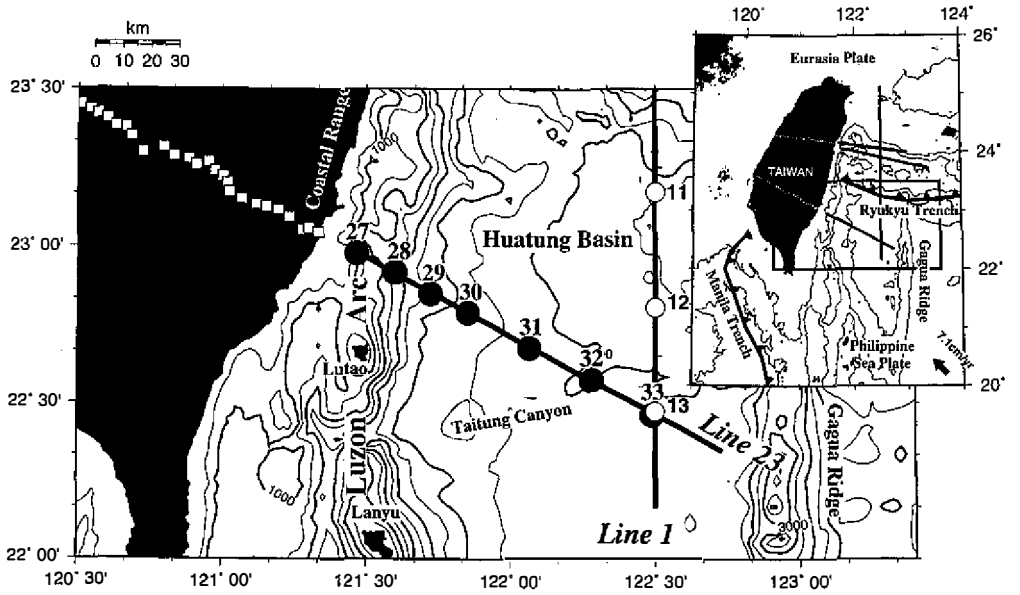

Fig. 1. OBS survey offshore southeastern Taiwan was conducted by R/V Maurice Ewing and R/V Ocean Researcher I during September 1995. Black and white circles indicate the OBS locations of Lines 23 and 1, respectively. Contour interval of the bathymetry data (Hsu *et al.*, 1996) is 500 meter.

out in September 1995 to investigate the deep structures and geodynamic processes of the arc-continent collision zone offshore southeastern Taiwan (Liu *et al.*, 1995; Wang *et al.*, 1996b; Yang *et al.*, 1996; Lin *et al.*, 1997; Yeh *et al.*, 1998). The preliminary results of this survey show that the oceanic basement of the western PSP beneath the Huatung Basin generally deepens westward east of the Luzon Arc (Chen, 1996; Yang *et al.*, 1996; Hetland and Wu, 1998; Yeh *et al.*, 1998). The aims of this paper are to further understand deformation of the shallow structures, the crustal velocity variation of the western PSP, and their relation to the arc-continent collision from the seismic survey offshore southeastern Taiwan.

2. OBS REFRACTION SURVEY

In the summer of 1995, a combined Ocean Bottom Seismometer (OBS) and multi-channel seismic (MCS) survey was conducted offshore eastern Taiwan with OBSs deployed from R/V Ocean Researcher I and an air-gun array and a multi-channel streamer from R/V Maurice Ewing. The seismic survey was designed to investigate the tectonic structures of the southwestern Ryukyu subduction zone (Wang *et al.*, 1996a and 1996b), the Ryukyu forearc system (Wang and Chiang, 1998; McIntosh and Nakamura, 1998), the western PSP (Yang *et al.*, 1996) and their interactions.

An OBS/MCS line (Line 23), lying in a NW-SE direction and having 7 OBSs (black circles in Figure 1), was acquired for exploring the crustal structures of the western PSP. The seismic line crosses the Luzon Arc, Huatung Basin and Taitung Canyon, and ends near the western edge of the Gagua Ridge with the total length of about 150 km. The north-south variation of the crustal structure beneath the Huatung Basin can be seen from the southern portion of OBS Line 1 (Wang *et al*, 1996a). OBS stations along Line 1 are denoted by white circles in Figure 1. The intersection of Line 1 and Line 23 at OBS stations 13 and 33 can provide more constraints for building the velocity models along both lines.

In this paper, we describe a velocity-depth model derived from OBS and MCS data and discuss its implications for the Luzon Arc and the western PSP offshore southeastern Taiwan. It is hoped that, by combining the velocity structures from both OBS Line 23 in this study and the land stations (white squares in Figure 1) across southern Taiwan (Chen, 1996; Lin *et al.*, 1997; Yeh *et al.*, 1998), we can provide better constraints on the crustal structures of the Taiwan Orogeny and new insights into the mountain building processes of Taiwan.

3. OBS DATA PROCESSING

OBS data processing in this study includes first arrival picking, velocity model building, ray tracing and travel-time inversion. These processing procedures are described as follows.

3.1 Initial Processing

By using an interactive software, OBSTOOL (Christeson, 1995), OBS raw data are processed through timing correction, station relocation, conversion to SEG-Y format, band-pass filtering, gain over offset and selection of the refracted and reflected arrivals. Figures 2(a)-(c) display the processed OBS data from stations 30, 31 and 32, respectively. The near-offset (<40 km) signals of OBS data in Figure 2 are generally clear and readily picked. However, as the offset increases, the signals become weaker. Signals refracted through the sediment (Ps) and the crust (Pg) are used to constrain the velocity in the model. These signals are generally strong and arrive early as shown in Figures 2(a)-(c). We also identify many arrivals refracted in the upper mantle (Pn). These arrivals and a few deep reflections (PmP) are used to determine crustal thickness.

3.2 Building a Starting Velocity Model

It is sufficient to build a shallow velocity model, based on the bathymetry (Figure 1) and the stacked MCS data (Figure 3), along the seismic profile. Several horizontal layers, with increasing velocity for deeper layers, are set in the starting model of the shallow structures. Four interfaces are readily identified from Figure 3. The uppermost interface, the seabed, shows that the depth of the sea floor increases toward the southeast. The two-way time of the water-bottom reflections increases from 2.5 sec at the northwest end to 6.5 sec at a distance of 90 km from the northwest end. The seabed is almost smooth at distances greater than 90 km

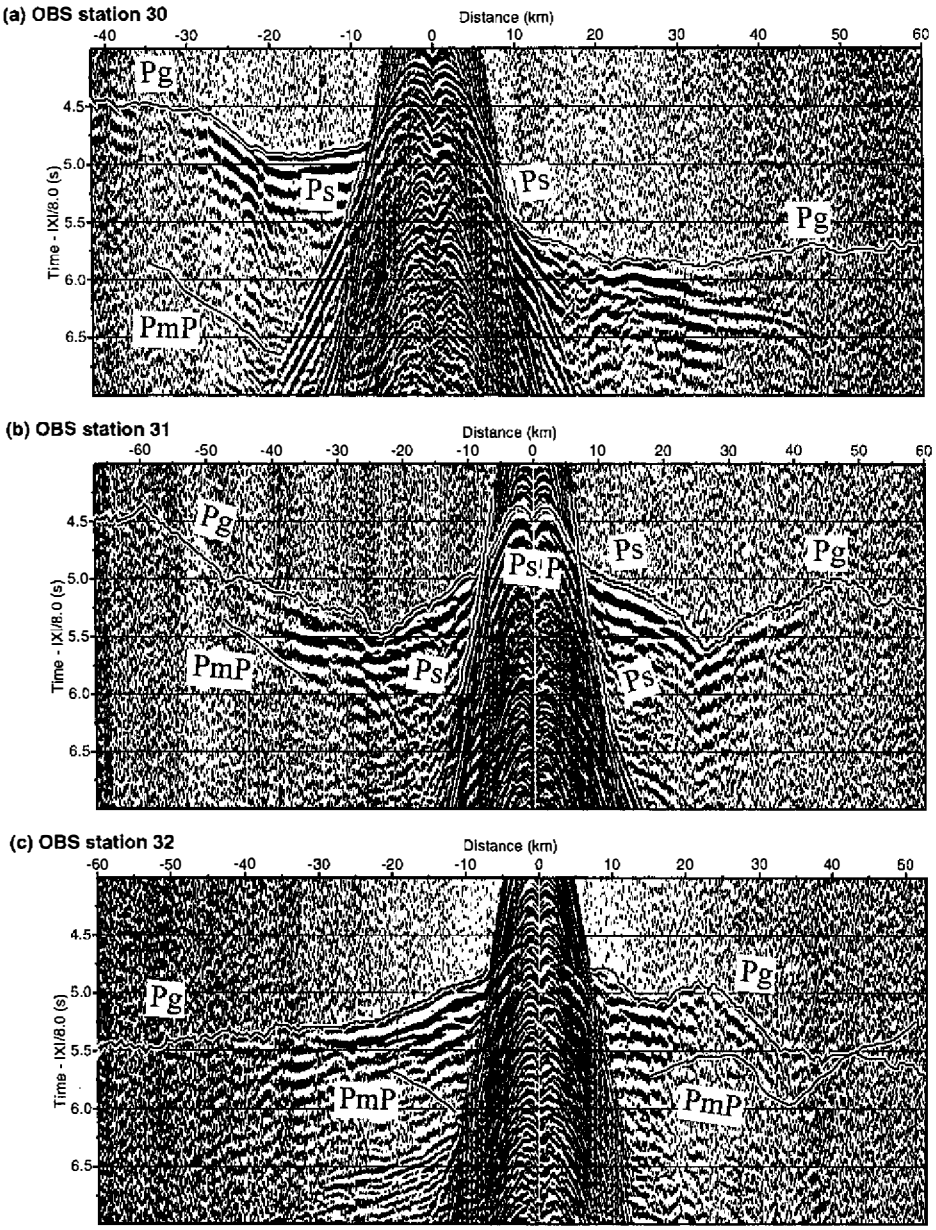

Fig. 2. Picked travel times of OBS data from vertical channel of (a) the station 30 (b) station 31 and (c) station 32. Seismic traces have been scaled to balance their amplitudes and a reduced velocity of 8 km/sec has been applied. Picks of four phases, Ps, Pg, PsP and PmP, indicate refracted signals from sediment, refracted signals from the crust, reflected signals from the sediment, reflected signals from the Moho, respectively.

except for a depression at a distance of 96 km (Taitung Canyon) and near the two ends (western edge of the Gagua Ridge). After travel-time inversion of the shallow velocity model (described in the next section), we build horizontal layers with the increasing velocity for the starting velocity model of the deep structures. The deep velocity model is derived using again the travel-time inversion described below.

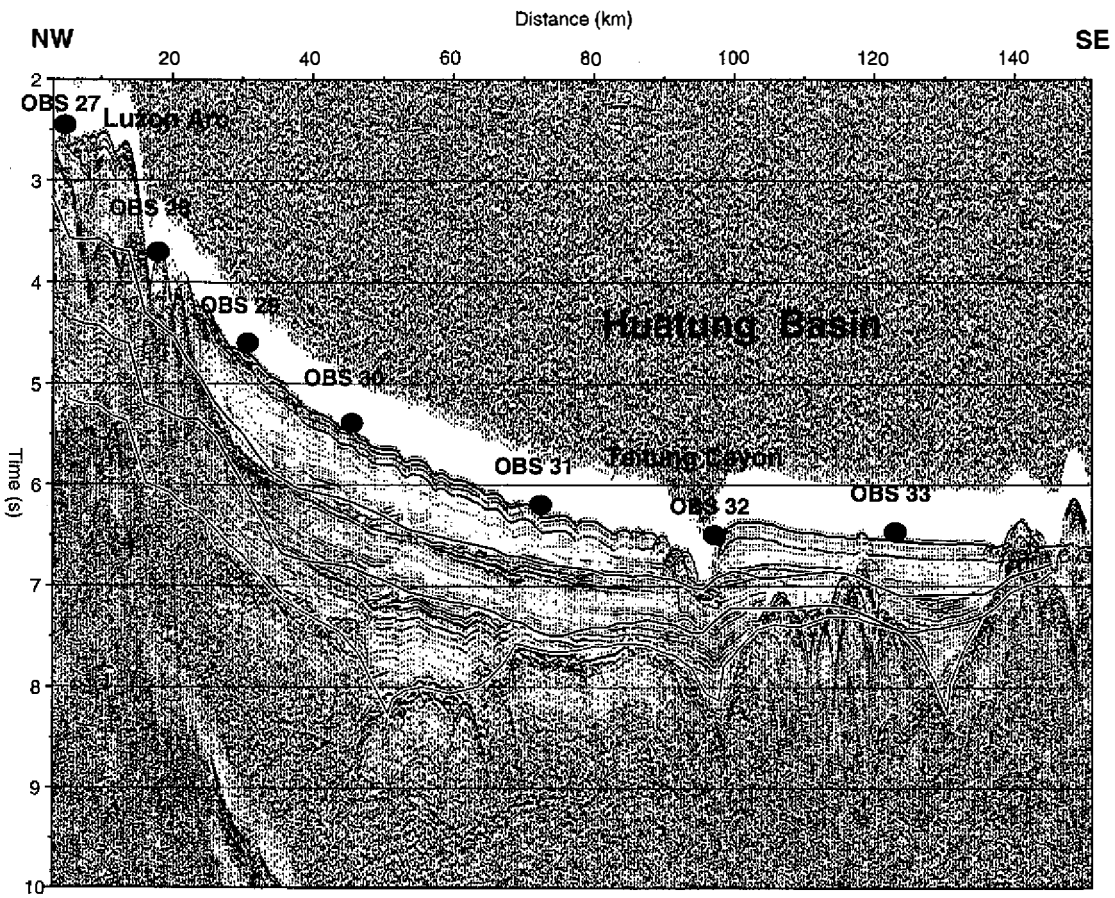

Fig. 3. Calculated travel times of the normal incidence (solid lines) from the final OBS velocity model are fitted well with the stacked MCS data for Line 23. From the top to the bottom, four interfaces are displayed. First interface is seabed while the sediment is between the first and third interfaces. Bottom of the compacted sediment as the fourth interface shows that a deep basement appears at distance of 50~60 km from the northwestern end, and two depressions are displayed below the Taitung Canyon and at distance of 130 km from the northwestern end, respectively.

3.3 Ray Tracing and the Travel-time Inversion

We comput travel times of tracing the reflected and refracted rays in the starting velocity model. Differences of the calculated and picked travel times are then considered in the inversion (Zelt and Smith, 1992) to update the velocity model. If the calculated and picked travel times do not fit well after several inversions, we modify the starting model, re-pick the far-offset travel times and re-start the inversion. The modifications are especially needed for deep structures and far-offset travel times because they are less certain.

In this paper, the velocity model is built from the shallow to the deep structures successively to ensure good travel-time fits at each step. Figures 4(a)-(c) show the ray coverage from the shallow to the deep structures of the final model while Figure 4(d) demonstrates the travel-time fit. The solid lines and the vertical bars in Figure 4(d) are the calculated and picked travel times, respectively. The vertical bars for the far-offset (>40 km) signals are longer that indicates the high uncertainty of the picked travel times, e. g. PmP arrivals displayed by the green bars in Figure 4(d). However, as illustrated by the green and pink in Figure 4(c), reflected rays from the Moho between 30~125 km and refracted rays through the upper mantle between 45~125 km provide sufficient constraints to the depth of the Moho.

The RMS travel-time error and the number of picks in the travel-time inversion of the velocity model are 0.176 sec and 3770, respectively. If the mean value of the velocity in the model is assumed to be 5 km/sec, the RMS travel-time error of 0.176 sec corresponds to an error in the distance (or the depth) of 0.88 km. The large number of picks in the travel-time inversion indicates that numerous rays penetrating the shallow and deep structures in Figures 4 (a)-(c) constrain well to the velocity model. Therefore, the error of the geometry and the resolution of the velocity model in this paper are acceptable.

4. RESULTS AND DISCUSSIONS

According to the OBS velocity model of the shallow structures (Figure 5), the travel times of the normal incidence from the shallow interfaces are calculated as three solid lines in Figure 3 that generally fit the stacked MCS data well. In addition, the velocity gradient shown in Figure 6 is obtained from the velocity model in Figure 7(a) by applying the Fourier transform along the seismic profile. The strong gradient contrast in Figure 6 is comparable with the interfaces of the velocity model as displayed by the solid lines. In view of the stacked MCS data in Figure 3, the contrast of the velocity gradient in Figure 6 and the strong velocity contrast in Figures 5 and 7(a), four velocity contours at 1.51, 3, 4.5 and 7.8 km/sec are labeled as the interfaces in the velocity models of Figures 5 and 7(a).

Based on a water-wave velocity of 1.5 km/sec, the velocity contour of 1.51 km/sec in the model indicating the sea floor is consistent with the water-bottom reflections in the MCS data. It is suggested that velocity contours of 3 and 4.5 km/sec in Figure 5 are, respectively, the bottoms of the sediment and the compacted sediment that match two of the lower interfaces in Figure 3. In addition, the observed PmP arrivals, illustrated by the green bars in Figure 4(d), provide constraints with the depth of the Moho in the travel-time inversion. Since the velocities above and below the Moho are, respectively, about 7.7 and 8.0 km/sec in the modeling, the

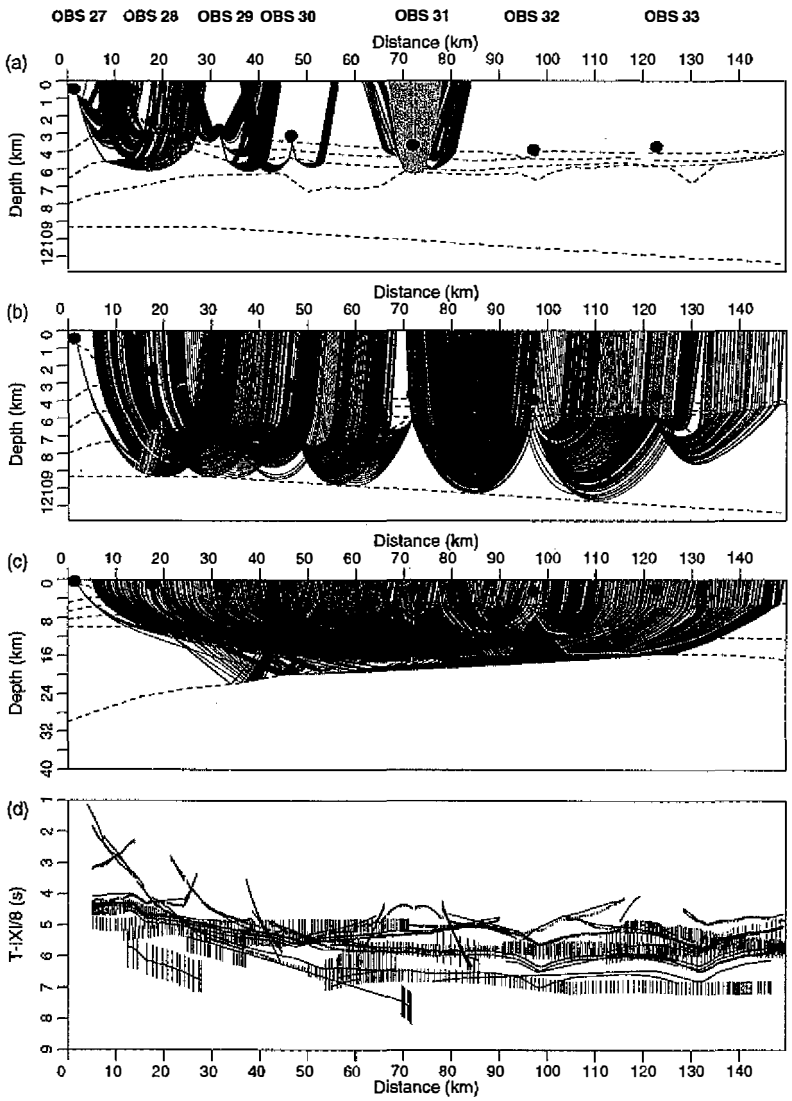

Fig. 4. (a) Reflected and refracted rays in the sediment of the shallow velocity model. (b) Refracted rays in the upper crust of the velocity model. (c) Refracted rays in the lower crust of the deep velocity model. (d) Calculated travel times (solid lines) fit well with the picked OBS data (vertical bars). Uncertainty of the picked arrival is denoted by half length of the vertical bar in seconds. Length of the vertical bars for near-offset (<40 km) signals is short, because OBS signals are readily picked. As offset increases, uncertainty of OBS signals increases and the length of the vertical bars is longer. Uncertainty of the reflection from the Moho (PmP) is generally high with the length of the vertical bars about 1 sec.

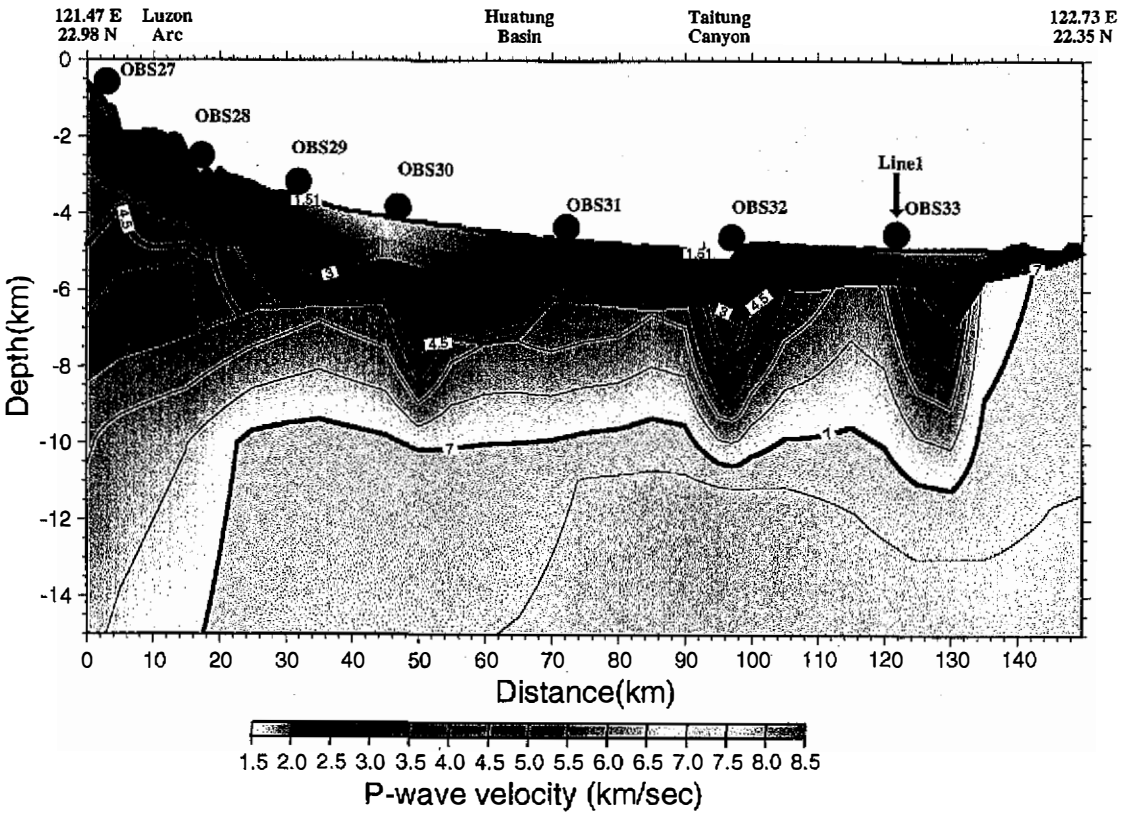

Fig. 5. Shallow model of the P-wave velocity. Three velocity contours of 3, 4.5 and 7 km/sec are labeled as bottoms of the sediment, compacted sediment and upper crust, respectively. Strong variation of the sea floor and deformation in the compacted sediment near the coast most likely resulted from arc-continent collision. Three depressions, deep basement beneath OBS stations 30 and 31, narrow basement trough beneath the Taitung Canyon and long-wavelength bending of the oceanic crust near the western edge of the Gagua Ridge, are found in the velocity model. Anomalously low velocity in the upper crust has also been identified beneath the Taitung Canyon and near the Gagua Ridge.

velocity contour of 7.8 km/sec in Figure 7(a) indicates as the Moho. Furthermore, a convex curve with high velocity gradients, from about a 30 km depth at the northwestern end of the model to about a 16 km depth at the southeastern end of the model in Figure 6, is consistent with the velocity contour of 7.8 km/sec in Figure 7(a) that also leads to 7.8 km/sec as the Pn velocity.

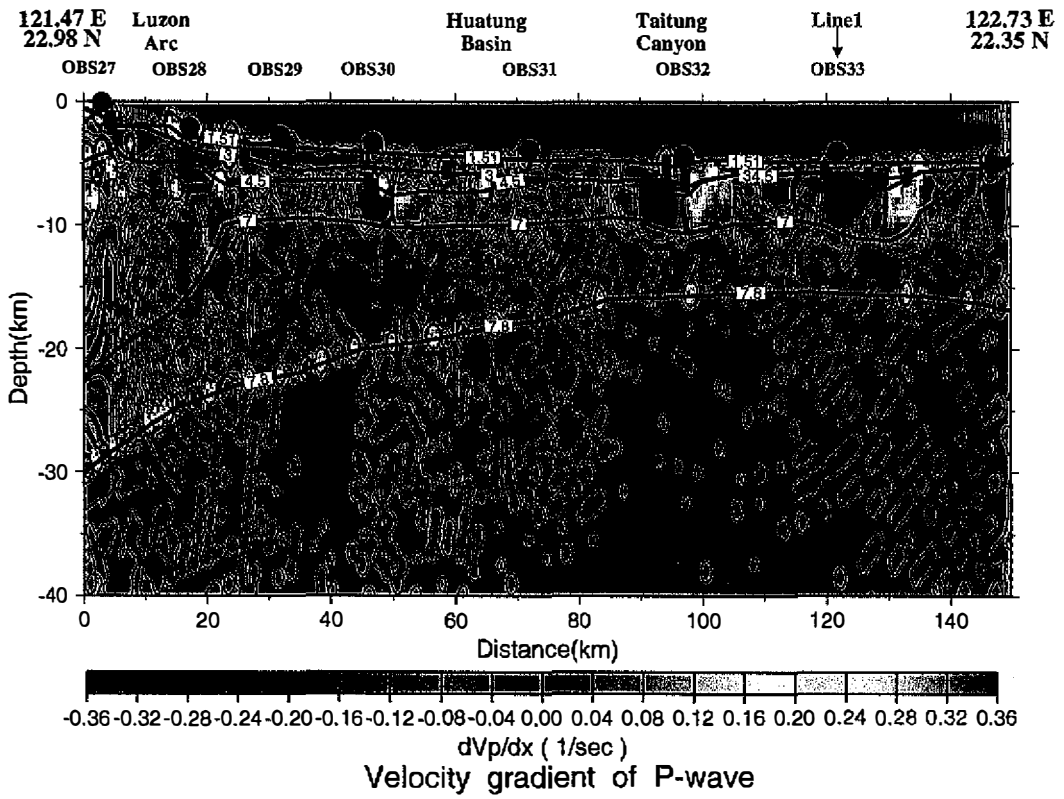

Fig. 6. Gradient of the P-wave velocity derived from applying Fourier transform of the velocity model along the seismic profile. Large gradient implies the strong variation of the velocity. Solid circles and solid lines indicate OBS locations and velocity interfaces, respectively.

4.1 Sediment (Vp = 1.51~3 km/sec)

Figure 5 displays only a thin layer of low velocity sediment below OBS station 27, the closest OBS station to Taiwan. The thickness gradually increases from 0.5 km (below OBS station 28) to 1.6 km (below OBS station 29), and then remains at 1.6 km southeastward throughout the Huatung Basin and the Taitung Canyon. The sediment between OBS stations 32 and 33 is thinner (about 1 km thick). The thickness of the sediment further decreases southeastward toward the end of the line about to 0.2 km.

Thinner sediment at the two ends of the model in Figure 5 most likely results from the sharp slopes of the sea floor above the Luzon Arc and near the Gagua Ridge. In contrast, in the center of the model, the Huatung Basin accumulates thicker sediment. According to the bathymetry (Hsu *et al.*, 1996) in Figure 1, the sedimentary section beneath Line 23 comes mainly from the Taiwan mountain-belt through the Taitung Canyon.

4.2 Volcaniclastics and Compacted Sediment (Vp = 3~4.5 km/sec)

Since the Neogene depositions in the Coastal Range are mainly marine and partly volcaniclastic (Ho, 1988), the velocity layer between 3~4.5 km/sec is possibly composed of "volcaniclastics" and older sediments at distances of 0~70 km in Figure 5. The thickness of this section at the northwest side of the model is about 4 km and becomes thinner southeastward. Deformation of the sea floor and the deeper section within a distance of 23 km from the northwestern end are seen in Figure 5 and may result from the collision of the Luzon Arc and the EP. In addition, a deep basement between OBS stations 30 and 31 was found 7 km below the sea level as shown in Figure 5. The bottom and the vertical offset of the deep basement are 15 km wide and 1 km deep, respectively. Since shallow and deeper sedimentary sections above the deep basement are not deformed, it is implied that the deep basement was formed before the collision, probably during the Eocene/Oligocene. Hence, the volcaniclastics in the deep basement were filled by the sediment probably after 41 to 33 Ma, when the oceanic basement was formed owing to the collision of the western PSP and the EP (Hsu *et al.*, 1998).

No volcaniclastics exists southeast of OBS station 31 except for two compacted sediments with a thickness of 1.5 km below Taitung Canyon and a thickness of 1 km southeast of OBS station 33 as illustrated in Figure 5. These compacted sediments are interpreted to have been deposited in a narrow basement trough beneath the Taitung Canyon and the long-wavelength bending of the oceanic crust owing to the uplift of the Gagua Ridge (Karp *et al.*, 1997; Deschamps *et al.*, 1997). The narrow basement trough beneath the Taitung Canyon may result from the right-lateral strike-slip fault of an old N-S trending fracture zone in the Huatung Basin (Lee and Hilde, 1984; Hsu *et al.*, 1996; Sibuet and Hsu, 1997; Hsu *et al.*, 1998).

4.3 Crust (Vp = 4.5~7.8 km/sec)

In Figure 5, we found three depressions in the crust that may result in continuous deposition of the compacted sediments below OBS stations 30, 32 and 33. These phenomena have been confirmed in this paper by adjusting various velocities and depths below the depressions of the compacted sediment for the best travel-time fits. Furthermore, the three pairs of negative and positive gradients (denoted, respectively, by blue and green in Figure 6) demonstrate the existence of three depressions in Figure 5.

The crustal thickness of the western PSP increases northwestward from about 10 km near the Gagua Ridge to about 26 km below the Luzon Arc in Figure 7(a). The velocity contour of 7 km/sec is chosen as the boundary between the upper and lower crust because the velocity contours of less than 7 km/sec are dense as shown in Figure 5. In addition, according to Figure 6, the velocity contour of 7 km/sec fits well as the bottom of the anomalously low velocity in the upper crust. The bottom of the upper crust drops abruptly from a 10 km depth (between OBS stations 28 and 29) to about a 22 km depth (at the northwest end) northwestward in Figure 7(a). Similarly, the depth of the velocity contour of 7.5 km/sec (between the velocity contours of 7 and 7.8 km/sec in Figure 7(a)) increases northwestward from 12 km depth (beneath OBS station 31) to 28.5 km depth (at the northwest end).

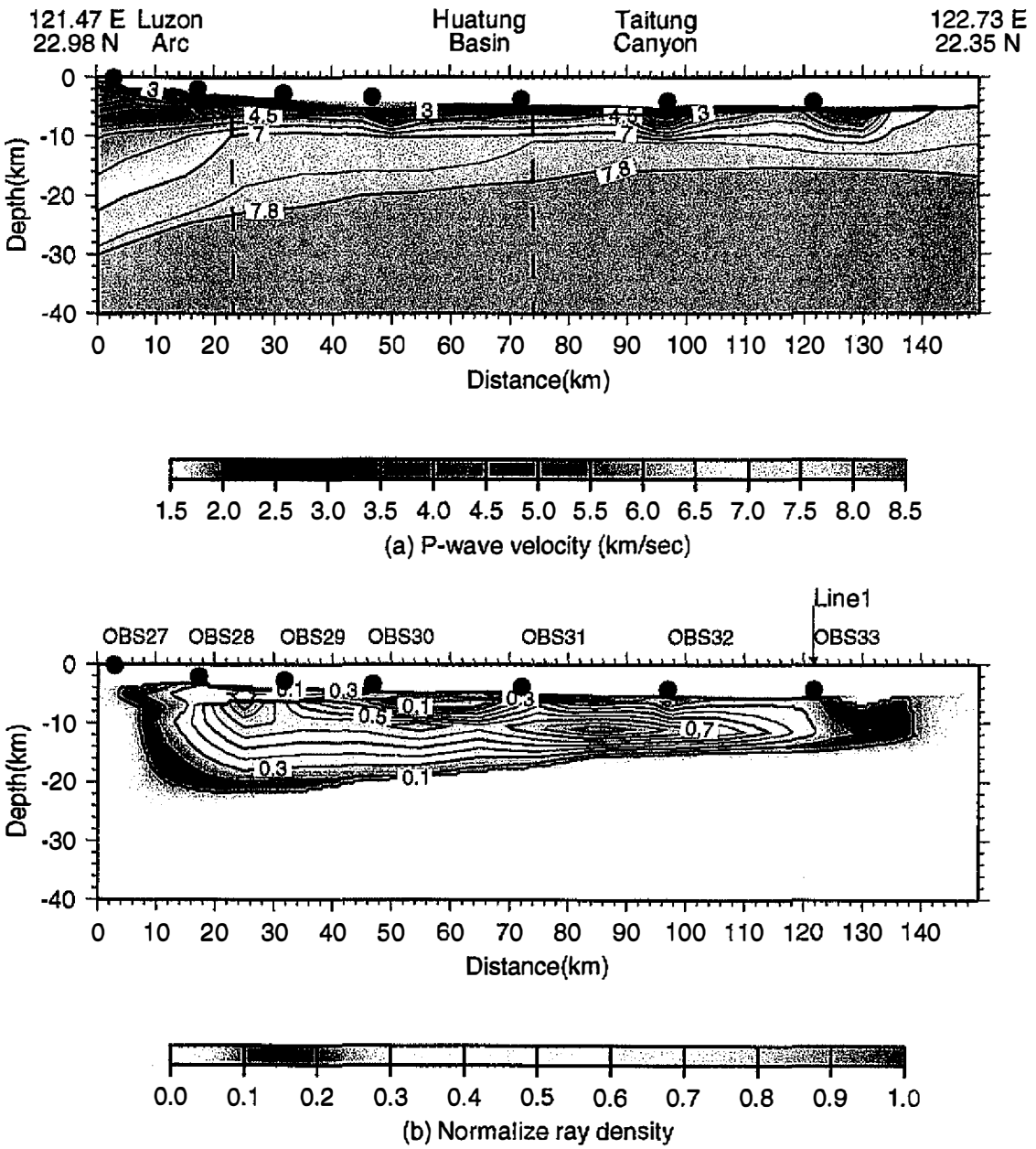

Fig. 7. (a) P-wave velocity model of OBS Line 23. RMS travel-time error of this model is 0.176 sec and number of picked travel times is 3770. (b) Normalized ray density of Line 23. Few rays penetrate beneath the Moho and at the two ends of this model.

According to the variation of the crustal thickness, the velocity model is divided into three portions. The first is with distances larger than 74 km, the second between 23~74 km and the third less than 23 km as illustrated by the dashed lines in Figure 7(a). The crustal thickness in the southeastern model (>74 km) and the thickness of the upper crust in the central model (23~74 km) are almost uniform at about 12 km and 4 km, respectively. However, the lower crust in the central model gradually thickens northwestward. In the northwestern model (<23 km), the upper crust gradually thickens northwestward while the thickness of the lower crust remains uniform. The maximum crustal thickness is about 24 km at the northwest side of the velocity model. In Figure 6, the gradient of the P-wave velocity within of 23 km of the northwest side of the model and the depth of 7~20 km is higher than that in the southeast. The contrast of the velocity gradient at a distance of 23 km implies that the eastern edge of the Luzon Arc is within the western PSP.

4.4 Moho (Vp = 7.8 km/sec)

Moho maintains a 16 km depth in the southeastern Huatung Basin and dips northwestward below the Luzon Arc at about 32 km depth as shown in Figure 7(a). The dipping angle of the Moho increases from 10 degree in the central basin to 17 degree below the Luzon Arc. The depth of the Moho (demonstrated in section 3.3) in this paper generally agrees with other studies (Chen, 1996; Hetland and Wu, 1998; Yang *et al.*, 1996; Yeh *et al.*, 1998).

5. CONCLUSIONS

High-quality OBS data have been acquired in a regional study comprising 7 OBS deployments along OBS Line 23 offshore southeastern Taiwan. By using travel-time inversion of OBS data and MCS data, we have built a high-resolution velocity model as shown in Figure 7(a). Figure 7(b) displays the normalized ray density of the travel-time modeling. The ray distribution is high for depths less than 20 km, but few rays can penetrate through and reflect from the Moho as illustrated by Pn and PmP arrivals in Figures 2(a)-(c), so that ray coverage is sparse in the lower crust of Figure 4(c).

Based on the velocity model established in this study, thick sediment from the Coastal Range have been deposited in the Huatung Basin. Three depressions (the deep basement at the east of the Luzon Arc, the narrow basement trough beneath the Taitung Canyon and the bending near the Gagua Ridge) have been found in Figure 5. Since the sediment is not deformed along the OBS line 23, the three depressions probably existed before the arc-continent collision.

On the basis of travel-time inversion in the paper, the oceanic crust around and below the sedimented depressions appears to have anomalously low velocity beneath the Taitung Canyon and near the Gagua Ridge. The former may be generated by the strike-slip fault (Hsu *et al.*, 1998; Schnürle *et al.*, 1998) while the latter may result from the uplift of the Gagua Ridge (Karp *et al.*, 1997; Deschamps *et al.*, 1997). The crustal thickness is almost uniform in the southeastern model (>74 km) of Figure 7(a). In the central model, the crustal thickness gradu-

ally thickens northwestward mainly from the lower crust. The upper crust at the northwest side (<23 km) is responsible for the thickening that the maximum crustal thickness reaches about 24 km. The variation of the crustal thickness in Figure 7(a) and the strong contrast of the velocity gradient in Figure 6 at a distance of 23 km imply the eastern edge of the Luzon Arc. Furthermore, the northwestward dipping of the Moho in the velocity model is also consistent with other studies (Chen, 1996; Yang *et al.*, 1996; Hetland and Wu, 1998; Hsu *et al.*, 1998; Yeh *et al.*, 1998). The mechanism of the crustal thickening in the western PSP is probably related to thrusting (Salzberg, 1996), intra-plate deformation or future subduction (Hetland and Wu, 1998) of the western PSP beneath the Luzon Arc.

Acknowledgments Chun-Shien Chiang and Ko-Chou Chang are thanked for instructing the first author in the packages of OBSTOOL and the travel-time inversion. Drs. C. S. Liu, C. S. Lee and S. K. Hsu's assistance in interpretation are much appreciated. This study was supported by National Science Council through NSC 86-2815-c-019-015-M (summer project for undergraduate students), NSC 85-2611-M-019-003 and NSC 86-2117-M-019-002-ODP.

REFERENCES

Chemenda, A. I., R. K. Yang, and J. C. Tang, 1997: Geodynamics of the Luzon-Taiwan-Ryukyu plate boundary: physical modeling. *Inter. Con. Sino-Amer. Sym. Tect. E. Asia, Taiwan,* 139.

Chen, B. Z., 1996: Interpretation and analysis of the onshore-offshore seismic profile across the southern Taiwan. Master's Thesis (in Chinese), Institute of Seismology, National Chung Cheng University, 82pp.

Christeson, G., 1995: OBSTOOL: Software for processing UTIG OBS data. University of Texas Institute for Geophysics, Technical Report, No. 134, 27pp.

Deschamps, A., S. Lallemand, and J. Y. Collot, 1997: The tectonic significance of the Gagua Ridge near Taiwan. *Inter. Con. Sino-Amer. Sym. Tect. E. Asia, Taiwan,* 142-143.

Hetland, E. A., and F. T. Wu, 1998: Deformation of the Philippine Sea Plate under the Coastal Range, Taiwan: Results from an offshore-onshore seismic experiment. *TAO*, **9**, 363-378.

Ho, C. S., 1988: An introduction of the geology of Taiwan: Explanatory text of the geological map of Taiwan. 2nd Ed., Ministry of Economic Affairs, ROC, 192pp.

Hsu, S. K., J. C. Sibuet, S. Monti, C. T. Shyu, and C. S. Liu, 1996: Transition between the Okinawa Trough backarc extension and the Taiwan collision: New insights on the southernmost Ryukyu subduction zone. *Mar. Geophys. Res.*, **18**, 163-187.

Hsu, S. K., C. S. Liu, C. T. Shyu, S. Y. Liu, J. C. Sibuet, S. Lallemand, C. Wang, and D. Reed, 1998: New gravity and magnetic anomaly maps in the Taiwan-Luzon region and their preliminary interpretation. *TAO*, **9**, 509-532.

Karp, B. Y., R. Kulinich, C. T. Shyu, and C. Wang, 1997: Some features of the arc-continent collision in the Ryukyu subduction system, Taiwan junction area. *In the Island Arc.*, **6**, 303-315.

Lee, C. S., and T. W. C. Hilde, 1984: Origin and evolution of the west Philippine Basin: A

new interpretation. *Tectonophysics,* **102**, 85-104.

Lin, C. H., Y. H. Yeh, B. S. Huang, R. C. Shih, H. L. Lai, C. S. Huang, S. S. Yu, H. Y. Yen, C. S. Liu, and F. T. Wu, 1997: Deep crustal structures inferred from wide-angle seismic data in Taiwan. *Inter. Con. Sino-Amer. Sym. Tect. E. Asia, Taiwan,* 155.

Liu, C. S., D. Reed, N. Lundberg, G. F. Moore, K. D. McIntosh, Y. Nakamura, T. K. Wang, A. T. Chen, and S. Lallemand, 1995: Deep seismic imaging of the Taiwan arc-continent collision zone. *EOS, Trans. Am. geophys. Un.*, **76**, 635.

McIntosh, K. D., and Y. Nakamura, 1998: Crustal structure beneath the Nanao forearc basin from TAICRUST MCS/OBS Line 14. *TAO*, **9**, 345-362.

Operto, S., 1996: RSTTI package: Ray based seismic travel time inversion. University of Texas Institute for Geophysics, Technical Report, No.148, 36pp.

Rau, R. J., and F. T. Wu, 1995: Tomographic imaging of lithospheric structures under Taiwan. *Earth Planet. Sci. Lett.*, **133**, 517-532.

Salzberg, D. H., 1996: Simultaneous inversion of moderate earthquakes using body and surface waves: Methodology and applications to the study of the tectonics of Taiwan. Ph. D. Thesis, State University of New York at Binghamton, 272pp.

Schnürle, P., C. S. Liu, S. E. Lallemand, and D. Reed, 1998: Structural controls of the Taitung Canyon in the Huatung Basin east of Taiwan. *TAO*, **9**, 453-472.

Seno, T., S. Stenin, and A. E. Gripp, 1993: A model for the motion of the Philippine sea plate with NUVEL-1 and geological data. *J. Geophys. Res.*, **98**, 17941-17948.

Sibuet, J. C., and S. K. Hsu, 1997: Geodynamics of the Taiwan arc-arc collision. *Tectonophysics*, **274**, 221-251.

Wang, T. K., K. D. McIntosh, Y. Nakamura and C. S. Liu, 1996a: OBS refraction survey and data processing offshore eastern Taiwan. *Proceeding of the Sixth Taiwan Symposium on Geophysics*, 37-46.

Wang, T. K., K. McIntosh, Y. Nakamura, and C. S. Liu, 1996b: OBS data refraction survey and imaging offshore eastern Taiwan. *EOS, Trans. Am. geophys.* Un., **77**, F 720.

Wang, T. K., and C. H. Chiang, 1998: Imaging of arc-arc collision in the Ryukyu forearc region offshore Hualien from TAICRUST OBS Line 16. *TAO*, **9**, 329-344.

Yang, Y. S., T. Lo, T. K. Wang, Y. Nakamura, and C. S. Liu, 1996: OBS data processing offshore southeastern Taiwan. *EOS, Trans. Am. geophys.* Un., **77**, F 732.

Yeh, Y. H., R. C. Shih, C. H. Lin, C. C. Liu, H. Y. Yen, B. S. Huang, C. S. Liu, P. Z. Chen, C. S. Huang, C. J. Wu, and F. T. Wu, 1998: Onshore/offshore wide-angle deep seismic profiling in Taiwan. *TAO*, **9**, 301-316.

Zelt, C. A., and R. B. Smith, 1992: Seismic traveltime inversion for 2-D crustal velocity structure. *Geophys. J. Int.*, **108**, 16-34.